



Trans. Nonferrous Met. Soc. China 23(2013) 2283-2293

Transactions of Nonferrous Metals Society of China

www.tnmsc.cn

# A review on in vitro corrosion performance test of biodegradable metallic materials

Zhen ZHEN<sup>1</sup>, Ting-fei XI<sup>1,2</sup>, Yu-feng ZHENG<sup>1,3</sup>

- 1. Center for Biomedical Materials and Tissue Engineering, Academy for Advanced Interdisciplinary Studies, Peking University, Beijing 100871, China;
  - 2. School of Information Engineering, Wenzhou Medical College, Wenzhou 325035, China;
- 3. Department of Materials Science and Engineering, College of Engineering, Peking University, Beijing 100871, China

Received 23 October 2012; accepted 1 March 2013

**Abstract:** Extensive in vitro corrosion test systems have been carried out to simulate the in vivo corrosion behavior of biodegradable metallic materials. Various methods have their own unique benefits and limitations. The corrosion mechanism of biodegradable alloys and in vitro corrosion test systems on biodegradable metallic materials are reviewed, to build a reasonable simulated in vitro test system for mimicking the in vivo animal test from the aspects of electrolyte solution selection, surface roughness influence, test methods and evaluation methodology of corrosion rate. Buffered simulated body fluid containing similar components to human blood plasma should be applied as electrolyte solution, such as simulated body fluid (SBF) and culture medium with serum. Surface roughness of samples and ratio of solution volume to sample surface area should be adopted based on the real implant situation, and the dynamic corrosion is preferred. As to the evaluation methodology of corrosion rate, different methods may complement one another.

Key words: biodegradable metallic material; in vitro corrosion test; Mg; Fe

#### 1 Introduction

Biodegradable metallic materials have received more attention in recent years. Due to biodegradability of metallic materials, negative effects brought by permanent existence of in vivo implants are reduced, such as inflammation, restenosis caused by cardiovascular stents and stress shielding induced by orthopedic implants. Mg alloys and Fe alloys are two kinds of biodegradable metals which are focused on by researchers. A great number of animal experiments [1-7] and clinical trials [8-11] have proved the safety and feasibility of biodegradable metals as implants, but meanwhile some shortcomings are also exposed. In spite of the immense potential of these two alloys, fast degradation rates of Mg-based biomedical implants and slow degradation rates of Fe-based biomedical implants in the physiological environment impose severe limitations in many clinical applications. In order to develop new kinds

of alloys and evaluate biocorrosion properties of the materials, a certain in vitro corrosion system should be established which can simulate degradable procedure of metal implants in vivo.

In vitro corrosion test mimics and evaluates in vivo degradable procedure by series of in vitro methods, such as electrochemical test, weight loss test and hydrogen evolution test [12]. Researchers build different in vitro simulating systems with various electrolyte solutions and diverse ratios of sample surface to solution volume, which lead to the incomparability of the data. Therefore, except for subjective treatment of the materials, such as element choice, surface coating, and processing technology, objective condition should be as same as possible and be close to in vivo condition. In order to establish a more suitable in vitro test system, four aspects were discussed as follows: 1) electrolyte solution selection; 2) surface roughness influence; 3) test methods: electrochemical test and immersion test; 4) evaluation methodology of corrosion rate.

Foundation item: Project (2012CB619102) supported by National Basic Research Program of China; Project (31070847) supported by National Natural Science Foundation of China

Corresponding author: Ting-fei XI; Tel: +86-10-62753404; Fax: +86-10-62753404; E-mail: xitingfei@pku.edu.cn DOI: 10.1016/S1003-6326(13)62730-2

## 2 Corrosion mechanism of biodegradable alloys

#### 2.1 Mg alloys

Mg dissolution in aqueous environments generally proceeds by an electrochemical reaction with water to produce Mg(OH)<sub>2</sub> and H<sub>2</sub> [13]. The overall corrosion reaction of Mg alloys has not yet been studied systematically. However, it is reasonable to expect that corrosion reactions of Mg alloys are similar to those of pure Mg. LI et al [14] reported that the main corrosion products of Mg alloys both in vivo and in vitro are Mg(OH)<sub>2</sub>. In vitro system, corrosion procedure mainly includes the chemical reactions as follows:

Mg 
$$Mg^{2+}+2e$$
 (1)

$$2H_2O+2e H_2 +2OH^-$$
 (2)

$$Mg^{2+}+2OH^{-} Mg(OH)_{2}$$
 (3)

LI et al [14] has revealed the corrosion processes and subsequent hydroxyapatite formation of Mg-Ca in a biocorrosion model at the alloy/aqueous solution interface, as shown in Fig. 1. This model can also be used to describe the corrosion process of other Mg alloys.

#### 2.2 Fe alloys

Different from the hydrogen evolution reaction of Mg alloys, Fe alloys appear oxidation absorption corrosion in aqueous environments. Based on the immersion test results of Fe in Hank's solution, the degradation mechanism is suggested by MORAVEJ et al [15] as follows.

When Fe is immersed in the solution or exposed to the solution flow, it is oxidized to Fe<sup>2+</sup> based on the following reaction:

Fe 
$$Fe^{2+}+2e^{-}$$
 (4)

Some of  $Fe^{2+}$  can be transformed to  $Fe^{3+}$  under the condition of alkaline pH and the oxygen environment of Hank's solution, and  $Fe(OH)_3$  is produced:

$$1/2O_2 + H_2O + 2e^- \quad 2OH^-$$
 (5)

$$Fe^{2+} + 2OH^{-}$$
  $Fe(OH)_2$  (6)

$$Fe^{2+}$$
  $Fe^{3+} + e^{-}$  (7)

$$Fe^{3+} + 3OH^{-} Fe(OH)_{3}$$
 (8)

As the solution is aerated and in the presence of chloride ions,  $Fe(OH)_3$  is hydrolyzed and goethite ( $\alpha$ -FeO(OH)) precipitates.

Fe(OH)<sub>2</sub> will then react with a part of FeO(OH) and magnetite is formed:

$$Fe(OH)_2 + 2FO(OH) \qquad Fe_3O_4 + H_2O \tag{9}$$

Precipitation of Ca and P element from solution along with hydroxide and oxide formed in the surface of Fe is responsible for the decrease after the first few days. Figure 2 shows the degradation mechanism of Fe–Mn alloy during the dynamic degradation test in modified Hank's solution.

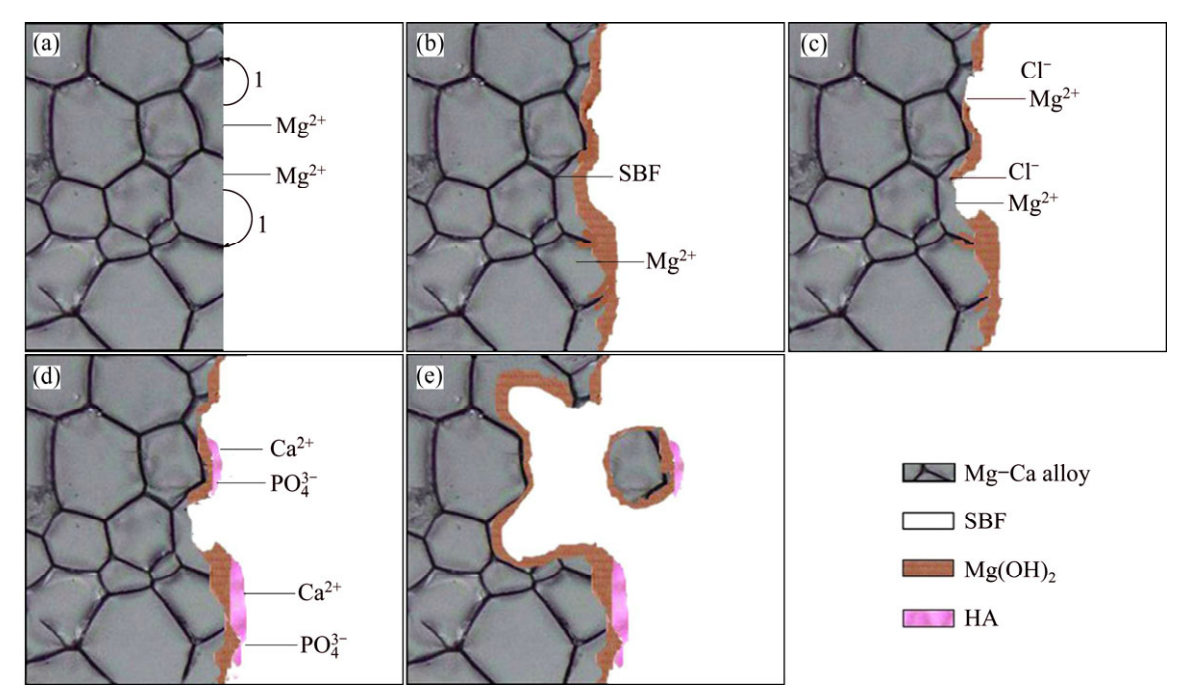


**Fig. 1** Schematic diagram of alloy/solution biocorrosion interface: (a) Galvanic corrosion between Mg and Mg<sub>2</sub>Ca phase; (b) Partially protective film covering surface of Mg<sub>2</sub>Ca alloys; (c) Adsorption of chloride ions to transform Mg(OH)<sub>2</sub> into MgCl<sub>2</sub>; (d) Hydroxyapatite formation by consuming Ca<sup>2+</sup> and PO<sub>4</sub><sup>3-</sup>; (e) Disintegrated particle-shape residues falling out of bulk substrate [14]

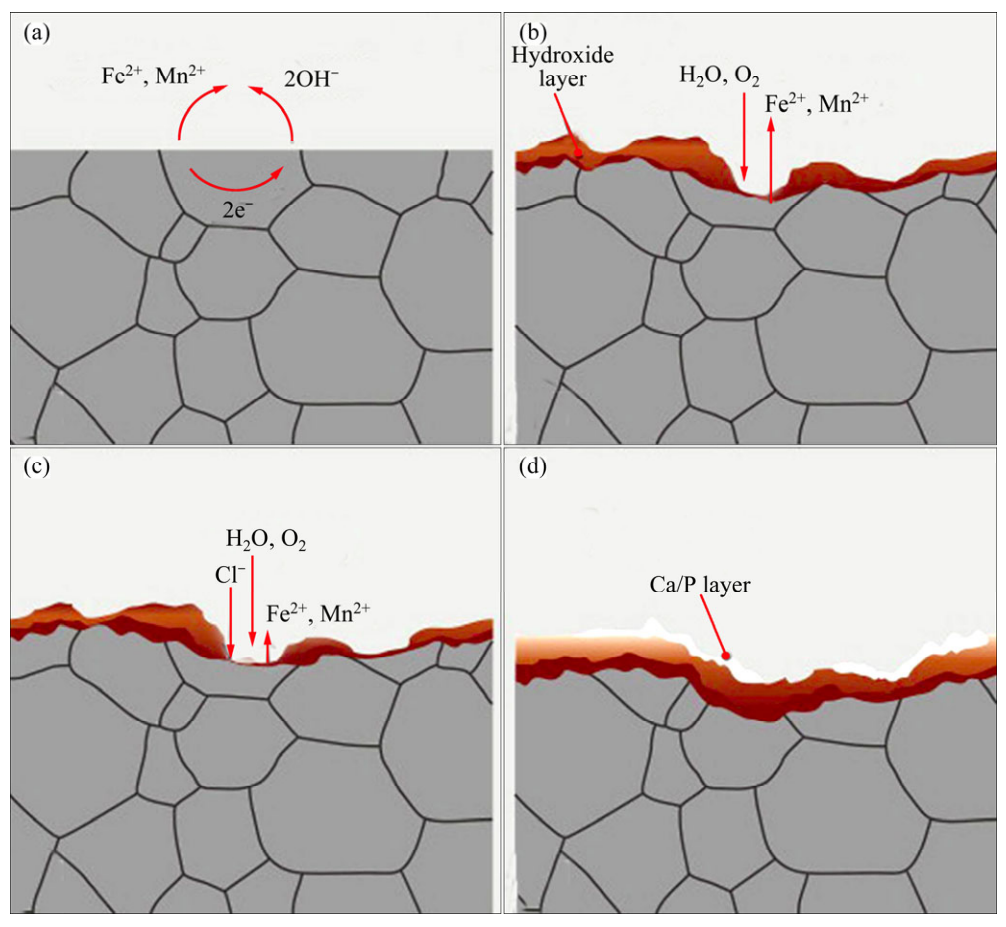


**Fig. 2** Illustration of corrosion mechanisms for Fe–Mn alloys: (a) Initial corrosion reaction; (b) Formation of hydroxide layer; (c) Formation of pits; (d) Formation of calcium/phosphorus layer

#### 3 In vitro corrosion test systems

#### 3.1 Electrolyte solution selection

To obtain the in vivo corrosion data via in vitro test, the most important factor is a suitable electrolyte solution system. Various solution systems have been used in the last ten years to mimic the body fluid. The main types of solution include: 0.9% NaCl aqueous solution, SBF (simulated body fluid), Hank's, PBS (phosphate buffered saline), DMEM and so on. Table 1 summarizes the composition of diverse simulated body fluid.

Materials show different corrosion behaviors in different solutions. Table 2 lists the electrochemical data of AZ91 alloys in various simulated body solutions. Taking AZ91D for example, the corrosion current density ( $J_{corr}$ ) (22.5  $\mu$ A/cm<sup>2</sup>) in 0.9% NaC1 aqueous solution tested by YAO et al [20] is less than that (297  $\mu$ A/cm<sup>2</sup>) in Hank's tested by SONG et al [21] by one order of magnitude. Even in the similar solutions, results may have great disparity. In m-SBF the  $J_{corr}$  is 65.7  $\mu$ A/cm<sup>2</sup> [17], while in m-SBF it is 0.705  $\mu$ A/cm<sup>2</sup> [22]. So

a certain composition of electrolyte solution is essential to the test system.

Table 1 Composition of diverse simulated body fluid

Solution	Composition		
DMEM	Dulbecco's modified eagle's medium		
Hank's	8.0 g/L NaCl, 0.4 g/L KCl, 0.14 g/L CaCl <sub>2</sub> , 0.35 g/L NaHCO <sub>3</sub> , 1.0 g/L C <sub>6</sub> H <sub>6</sub> O <sub>6</sub> (glucose), 0.1 g/L MgCl <sub>2</sub> ·6H <sub>2</sub> O, 0.06 g/L MgSO <sub>4</sub> ·7H <sub>2</sub> O, 0.06 g/L KH <sub>2</sub> PO <sub>4</sub> , 0.06 g/L Na <sub>2</sub> HPO <sub>4</sub> ·12H <sub>2</sub> O	[16]	
m-SBF	5.403 g/L NaCl, 0.504 g/L NaHCO <sub>3</sub> , 0.426 g/L Na <sub>2</sub> CO <sub>3</sub> , 0.225 g/L KCl, 0.230 g/L K <sub>2</sub> HPO <sub>4</sub> ·3H <sub>2</sub> O, 0.311 g/L MgCl·6H <sub>2</sub> O, 100 mL 0.2 mol/L NaOH, 17.892 g/L HEPES, 0.293 g/L CaCl <sub>2</sub> , 0.072 g/L Na <sub>2</sub> SO <sub>4</sub>	[17]	
SBF	8.035 g/L NaCl, 0.355 g/L NaHCO <sub>3</sub> , 0.225 g/L KCl, 0.231 g/L K <sub>2</sub> HPO <sub>4</sub> '3H <sub>2</sub> O, 0.311 g/L MgCl <sub>2</sub> ·6H <sub>2</sub> O, 39 mL 1.0 mol/L HCl, 0.292 g/L CaCl <sub>2</sub> , 0.072 g/L Na <sub>2</sub> SO <sub>4</sub> , 6.118 g/L Tris, 0-5 mL 1.0 mol/L HCl	[18]	
PBS	0.20 g/L KCl, 0.20 g/L KH <sub>2</sub> PO <sub>4</sub> , 8.00 g/L NaCl , 1.15 g/L Na <sub>2</sub> HPO <sub>4</sub>	[19]	

**Table 2** Electrochemical data of AZ91 alloys in various simulated body solutions

Alloy	Roughness	Solution	$arphi_{ m corr}$ /	$J_{\rm corr}/$ ( $\mu { m A \cdot cm}^{-2}$ )	Ref.
		Blood plasma	-1.53		
		NaCl	-1.518		
AZ91	4000	NaCl+K <sub>2</sub> HPO <sub>4</sub>	-1.774		[23]
		NaCl+K <sub>2</sub> HPO <sub>4</sub> + NaHCO <sub>3</sub>	-1.789		
AZ91	4000	SBF	-1.836	3.75	[22]
AZ91	2400	m-SBF	-1.713	65.7	[17]
AZ91D	1000	Hank's	-1.36	297	[21]
AZ91D	1	0.9% NaCl	-1.528	22.56	[20]
AZ91E	0.5 μm diamond	Hank's	-1.593	4.927	[24]

YAMAMOTO and HIROMOTO investigated the effects of inorganic salts, amino acids and proteins on the degradation of pure Mg in vitro. Six types of solutions were used for immersion tests: plasma, NaCl, NaCl+HEPES, NaCl+NaHCO<sub>3</sub>, Earle(+), E-MEM, and E-MEM+FBS. The results illustrate that protein adsorption onto Mg disk surface has a significant effect on retardation of Mg dissolution. This may be attributed to the adsorption of proteins, which makes insoluble salt layer dense or more effective as a barrier against corrosion. But amino acids and some organic chelating compounds can form a complex with metal cation, which accelerates the dissolution of metal. ZENG et al [26] have obtained the same conclusion that the addition of bovine serum albumin (BSA) significantly shifts open-circuit potential toward a more positive value in SBF and tends to retard localized corrosion. XIN et al [23] have studied the influence of aggressive ions on degradation behavior of biomedical Mg alloy in physiological environment. They conclude that OH can raise localized corrosion and stabilize the corrosion product Mg(OH)2, but Mg(OH)2 layer is loose and cannot provide sufficient protection. In addition, chloride ions on surface can transform the formed Mg(OH)2 into soluble MgCl<sub>2</sub>, while HCO<sub>3</sub> and HPO<sub>4</sub><sup>2-</sup> transform Mg(OH)2 into the more stable giorgiosite Mg<sub>5</sub>(CO<sub>3</sub>)<sub>4</sub>(OH)<sub>2</sub>5H<sub>2</sub>O and Mg<sub>3</sub>(PO<sub>4</sub>)<sub>2</sub>, respectively. High pH accelerates the precipitation of Mg phosphate and carbonate, and also stabilizes Mg(OH)2. These results have been verified by other studies as well. The corrosion rate of magnesium in HPO<sub>4</sub><sup>2-</sup>-scarce SBF is twice that in normal SBF [27], and HIROMOTO et al [28] studied the influence of pH on the corrosion property of pure magnesium in borate buffer solutions, which illustrates pH would affect the stability of  $Mg(OH)_2$ .

To sum up, the influence of inorganic ion on the corrosion mechanism of Mg alloys is as follows:

Mg 
$$Mg^{2+}+2e$$
 (10)

$$2H_2O+2e H_2 +2OH^-$$
 (11)

$$Mg^{2+}+2OH^{-} Mg(OH)_{2}$$
 (12)

$$Mg(OH)_2+CI^- Mg^{2+}+CI^-+2OH^-$$
 (13)

$$Mg(OH)_2 + HCO_3^- Mg_5(CO_3)_4(OH)_2 \cdot 5H_2O$$
 (14)

$$Mg^{2+} + HPO_4^{2-} MgHPO_4$$
 (15)

To conclude, both inorganic ion and organic components have a significant influence on the degradation procedure of metal alloys, so composition of the solution must be chosen cautiously. A buffer electrolyte solution containing the similar component to human blood plasma should be used to convey the in vitro biodegradation test.

#### 3.2 Influence of surface roughness

Various surface treatments are applied to improve the corrosion property of biomaterials. These treatments, such as blast sanding, coating or oxidation, are intentional changes to deal with metallic materials, but the influence of surface roughness on the corrosion property is usually ignored. Grinding processes differ form 1000 mesh [27,29], 1200 mesh [16,30], 2000 mesh [12,31] to 4000 mesh papers[19,32] and follow diamond paste polishing with different particle sizes [24,33]. However, surface roughness impacts the corrosion rate of materials. Surface treatment like mechanical polishing, electrolytic polishing and picking will enhance their corrosion resistance, while the rough surface will increase the corrosion rate [34]. Meanwhile, surface roughness has effect on proliferation, differentiation, and protein synthesis of human osteoblast cells [35], and the cell secretions could affect the biodegradation of metallic materials conversely. Therefore, to biodegradation process of implants, the surface treatment of test samples should be as same as clinic products.

#### 3.3 Electrochemical test

Electrochemical test is a convenient and easy method to evaluate the corrosion property by testing the OCP (open circuit potential), polarization curves and EIS (electrochemical impedance spectroscopy) via a three-electrode system. The followings are some aspects that affect the corrosion results.

#### 3.3.1 Scanning rate of polarization curves

Potentiodynamic polarization measurement is the most popular method adopted by researchers for its convenience [12,14,16,17,19–24,26,30–32,36–51], but the difference of parameter selection can bring distinction.

One of the most important parameters is scanning rate. With the increase of scanning rate,  $J_{\text{corr}}$  rises and zero current potential shifts to more negative value. The reason is that when scanning rate is low, electrode system is in steady-state approximation. The speed of electron transfer is equal to that of electron consumption at this state, so an accurate zero current potential can be obtained. As scanning rate increases, the steady state of system is disturbed, and the speed of electron transfer is larger than that of electron consumption in cathode reaction, which leads to the accumulation of electrons on the surface of electrode and causes the negative shift of zero current potential [52]. In addition, the slower the scanning rate is, the clearer the peak of current density becomes. Therefore, the scanning rate of the potentiodynamic polarization measurement should be slow enough, and the testing time should be short. 0.5 mV/s or 1 mV/s is suggested.

#### 3.3.2 Frequency of EIS

In the test of EIS, the frequency range has an important effect on the spectra. If the electrode system is stable enough, the frequency should be low enough to make the measure time longer. On the other hand, if the electrode system is active, the surface character has changed during the long time test. The data have little significance in this situation. So the frequency should be higher to ensure a short time test. Therefore, the selection of a reasonable test frequency range according to the concrete conditions is fatal to getting object data [53]. The range of 100 kHz-10 mHz is generally adopted [17, 21-23,32,37,40]. The lowest frequency is set at 10 mHz in order to reduce the time and potential noise interference. The EIS measurement may be affected by phase shifts from the potentiostat in high frequency region, so the upper frequency limit is set at 100 kHz [23].

#### 3.4 Immersion test

Immersion test is also a common method to evaluate the corrosion properties of biodegradable metallic materials. According to ISO 10993-15 [54] (Biological evaluation of medical devices-Part 15: Identification and quantification of degradation products from metals and alloys), and ASTM G31-72 [55] (Standard practice for laboratory immersion corrosion testing of metals), tested materials are degraded in chemical solutions, and the corrosion products are analyzed by a series of methods. ISO 10993-15 indicates that test cell should be tightly closed to prevent evaporation and maintained at 37 °C for 7 d and then is analyzed. Factors which affect the results contain the ratio of solution volume to sample surface area (V/S), the flow rate, the immersion time and the evaluation method of corrosion rate.

3.4.1 Ratio of solution volume to sample surface area (V/S)

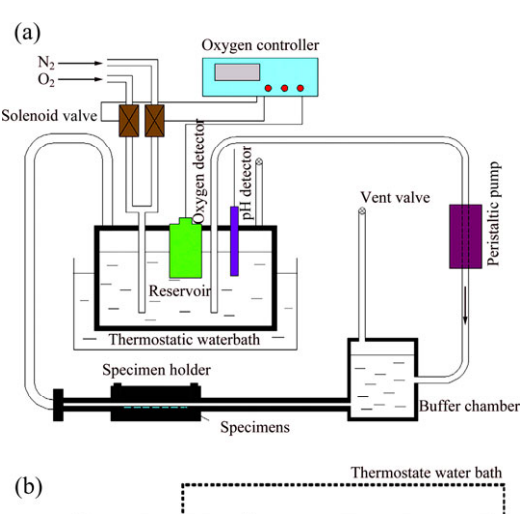
The minimum value of V/S recommend by ASTM G31—72 are 20 mL/cm<sup>2</sup> and 40 mL/cm<sup>2</sup>, to ensure the volume of test solution large enough to avoid any appreciable change in its corrosion during the test, either through exhaustion of corrosive constituents or by accumulation of corrosion products that might affect further corrosion. To the contrary, according to ISO10993—15, the V/S should less than 1 mL/cm<sup>2</sup>. Various ratios of V/S were adopted in the immersion test [12,31,33,39-41,44,56,57], from 0.33 mL/cm<sup>2</sup> [57] to 500 mL/cm<sup>2</sup> [44]. YANG and ZHANG [12] have studied the influence of V/S ratio on materials corrosion rate by changing the ratio from 0.67 mL/cm<sup>2</sup>, 6.67 mL/cm<sup>2</sup> to 66.7 mL/cm<sup>2</sup>. The results listed in Table 3 show that V/S ratio significantly influenced the corrosion rate of magnesium alloy. Low ratio led to a high pH, which retarded the corrosion. However, when the ratio was high enough, such as 6.7, the effect was negligible. Selection of the simulated solution and the V/S ratio on the basis of bioenvironmental application would be very necessary. It was suggested that a high V/S ratio, such as 6.7, and a low V/S ratio, such as 0.67, should be selected to simulate the in vivo degradation behavior of magnesium bone screw in a bone marrow cavity and magnesium plant and screw in cortical bone or muscle tissue, respectively. Consequently, the V/S ratio should be considered in terms what are clinically relevant.

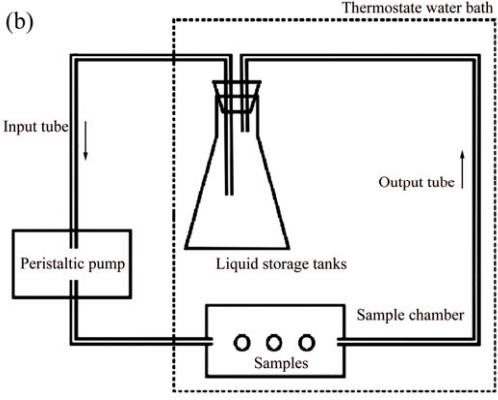
**Table 3** Influence of *V/S* ratio on corrosion rate of Mg-1Mn-1Zn in Hank's solution [12]

Alloy	V/S ratio/ (mL·cm <sup>-2</sup> )	Solution	Corrosion rate/ (mg·cm <sup>-2</sup> ·h <sup>-1</sup> )
Mg-1Mn-1Zn	6.7	Hank's	0.0032
Mg-1Mn-1Zn	66.7	Hank's	0.0058

#### 3.4.2 Flow rate of solution

According to the state of immersion solution, tests are divided into static immersion and dynamic immersion. In static immersion test, the samples are soaked in still solution, while in dynamic immersion test, the solution is flowing. Most reports adopt static immersion test to evaluate the corrosion property of metallic materials, yet some results show that data of in vitro corrosion cannot predict in vivo corrosion [36]. Therefore, a series of dynamic equipments are invented for better simulation of the in vivo environment. A Chandler-Loop [58,59] is adopted to simulate the corrosion environment of magnesium alloys for cardiovascular stents using human whole blood, and static immersion test in SBF is used as control. Overall, no correlation between blood and PBS data could be found. It is suggested that future studies for blood contacting devices should account for using more physiologically accurate test systems by using fresh human whole blood under flow conditions or improved SBF solutions. Shakers are also used to imitate the scour to samples of body fluid by adjusting the rotation speed [28,60]. HIROMOTO et al [28] have studied the corrosion procedure of pure magnesium in 0.6% (mass fraction) NaCl under divers rotation speed (1, 120, 1440 r/min), and found that the flowing of solution accelerates the corrosion process by reducing the deposition of corrosion products. It is concluded that flow rate of the test solution should be controlled depending on the implanted part of body. Some researchers develop devices driven by pump as shown in Fig. 3 [50,61,62]. The pressure of pump could be adjusted according to





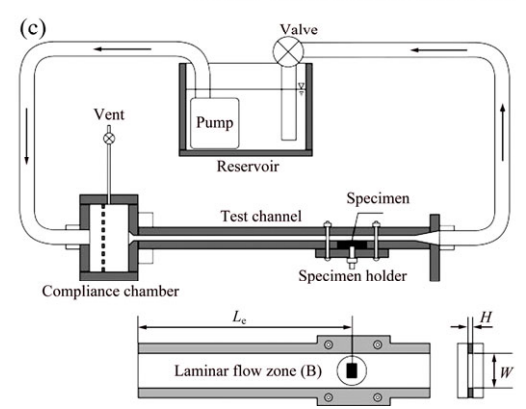


**Fig. 3** Diagram of dynamic corrosion test devices: (a) Ref. [50]; (b) Ref. [63]; (c) Ref. [62]

shear force on the surface of implants. As to the shear force, there is no agreement at the moment.

0.68 Pa [61] and 1.14 Pa [63] are both used as the stress of artery. The amplitude of shear stress has a strong influence on the corrosion process. When this stress is low, it protects the surface from localized corrosion. However, when it is very high, in addition to high uniform corrosion, some localized corrosion also occurs [62].

#### 3.4.3 Immersion time

The corrosion rate has been changing over time in immersion time. Figure 4 shows that the corrosion rate usually decreases as the time increases [33,44,57,64]. Therefore, the data of different immersion time could not be compared. Once the materials are implanted in human body, there will be many physical reactions on the surface of implants, such as protein absorption and cell adherence. The effect of protein adsorption and cell attachment on degradation performance must be studied in more detail [65]. Therefore, even if the initial simulated state is similar to the in vivo environment, it has changed far from the real situation over time. So the immersion time should be in a limited time.

#### 3.5 Evaluation methodology of corrosion rate

There are 4 methods to evaluation the corrosion rate of metallic materials: mass loss, hydrogen evolution, ion release concentration, and electrochemical corrosion current.

#### 3.5.1 Mass loss/gain

Mass loss/gain is the method to evaluate the corrosion rate by measuring the mass change of samples before and after immersion test. The sample is immersed in the corrosion medium for a period of time, after which the specimen is removed and the change in mass is measured. The following is the formula to calculate corrosion rate:

$$R = \frac{W}{At\rho} \tag{16}$$

where R is the corrosion rate, W is the change of mass, A is the original surface area exposed to the corrosive media, t is the exposure time, and  $\rho$  is the standard density of sample.

This evaluation method is simple, but the detailed operations are different. It is also important to consider the removal of corrosion product after immersion. Some researchers [36,40,64] just remove the samples from the solution, rinse them with distilled water, and weigh the samples. Others [49] try to move the surface corrosion products by brush. While the rest scientists [16,44,46,50, 56] clean samples by chemicals such as 180 g/L chromic acid to remove the corrosion products.

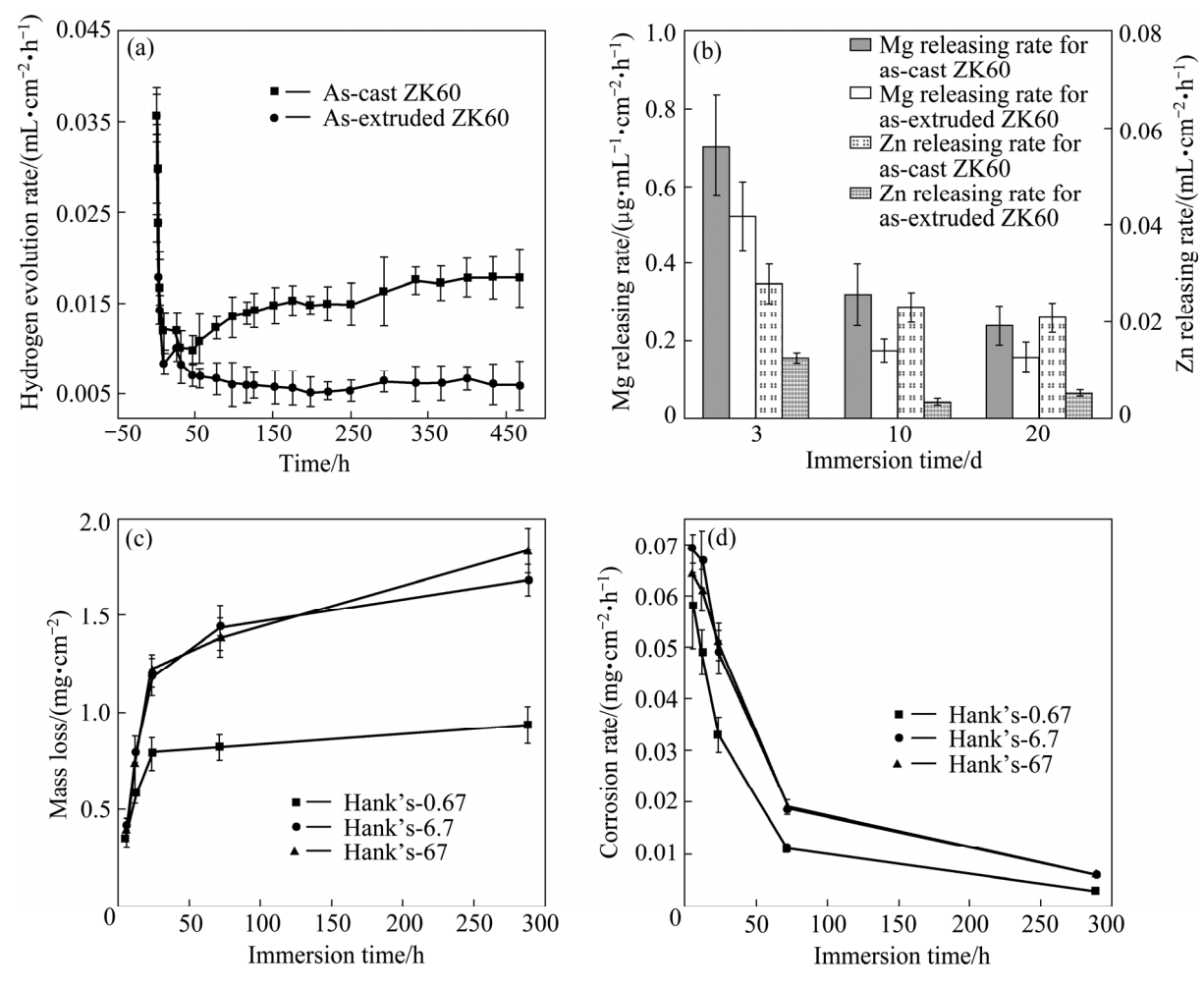
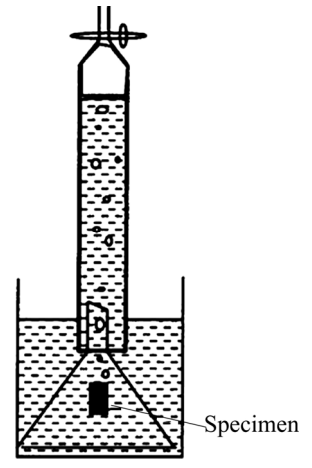


Fig. 4 Change of corrosion rates as a function of immersion time: (a), (b) Mass loss and average corrosion rate of Mg–Mn–Zn alloy in different solutions [12]; (c), (d) Hydrogen evolution rate and ion releasing rate in Hank's solution for as-cast and as-extruded ZK60 alloy [66]

These operations all have some shortcomings: 1) Brushing may destroy the matrix of the metals leaving scratches on the surface, which adds the mass loss. 2) Only washing with distilled water cannot remove all the corrosion products, leading to mass gain [36]. 3) Washing by chemical reagent also should be paid much attention to, preventing that the matrix reacts with chemicals during the long time washing. Apart from that, surface treated samples like coating or microarc oxidation should avoid chemical washing to prevent the reactions between surface composition and chemical regent. So in order to limit the man-made error, different methods should be applied.

#### 3.5.2 Hydrogen evolution

Hydrogen evolution can only evaluate the corrosion properties of metals which can elute gas when immersed in simulated body fluid, such as Mg alloys. The device to measure the corrosion rate by measuring the volume of hydrogen evolved is shown in Fig. 5 [67]. The principle is based on the corrosion reaction of magnesium, given by Eq. (17).



**Fig. 5** Schematic illustration of procedure to measure corrosion rate by measuring volume of hydrogen evolved [67]

As shown in Eq. (17), the dissolution of 1 mol Mg generates 1 mol  $H_2$ . According to the volume of  $H_2$  and Eq. (18), the corrosion rate could be calculated by substituting 1 mL  $H_2$ (=0.001083 g Mg) into Eq. (16).

Therefore, the measurement of  $H_2$  is equivalent to the measurement of mass loss of Mg:

$$Mg(s)+2H_2O(aq) \Longrightarrow Mg(OH)_2(s)+H_2(g)$$
 (17)

$$PV=nRT \tag{18}$$

where P is standard atmospheric pressure (Pa), V is volume of  $H_2$  (m<sup>3</sup>), n is the substance amount of the gas (mol), T is the temperature (K).

Different from mass loss experiments, hydrogen evolution measurement is a real-time dynamic observation of the corrosion procedure. So it can easily record the change trend of corrosion rate by multiple-time metering. Another point is that hydrogen evolution just reflects the cathode reaction of Mg, but other mechanisms of corrosion such as the detachment of noble second phase are ignored.

This simple and inexpensive method also has some limitations due to atmospheric pressure changes or possible hydrogen leakages from the experimental set-up. Furthermore, the stoichiometry of redox equation which produces elemental hydrogen is not fully understood and thus the volume of  $H_2$  cannot be directly correlated to the production of  $Mg^{2+}$  [68].

#### 3.5.3 Released ion concentration

The released ion concentration in the immersion solution is another way to calculate corrosion rate of metallic materials. The immersion solution is digested by adding acid, and inductively coupled plasma-atomic emission spectrometer is used to measure the ion concentration. The computation equation is given as follows [50]:

$$R = \frac{cV}{S_t} \tag{19}$$

where R is the corrosion rate, c is the ion release concentration, V is the volume of immersion solution, S is the original surface area exposed to corrosive media, and t is the exposure time.

This method has the same problem as mass loss method, which may lead to deviation if the surface corrosion products cannot be wholly removed into the solution.

### 3.5.4 Electrochemical corrosion current (ASTM-G102—89) [69]

The most common methods to determine the corrosion rate in vitro are gravimetric measurements and electrochemical measurements (linear polarization, electrochemical impedance spectroscopy). As a non-destructive method of microtomography, especially synchrotron-based microtomography, electrochemical corrosion test is introduced to obtain general corrosion rates by observing the time-dependent change in the metallic volume of the remaining implant [68]. The computation equation is as follows:

$$R = K \frac{J_{\text{corr}}}{\rho} m_{\text{e}} \tag{20}$$

where R is the corrosion rate, K is  $3.273 \times 10^{-3}$  mm·g/ ( $\mu$ A·cm·a),  $J_{corr}$  is the current density, and  $m_e$  is equivalent mass.

Mg alloys exhibit different corrosion rates by different corrosion tests, even for the same Mg alloy [68]. In most reports, similar trends of different samples can be observed. For example, YFANTIS et al [70] measured various Mg alloys by both electrochemical test and mass loss test in 0.1 mol/L NaCl, which finds that though corrosion rates calculated from the two methods differ by one order of magnitude, corrosion rate sequences of the alloys are the same as Table 4 shows.

To summarize, electrochemical test is a kind of accelerating corrosion method, which cannot simulate the true corrosion situation in vivo, but could be used as a basis of corrosion property. Methods of mass loss hydrogen evolution and ion release concentration also have certain defects. These methods should be cross-referenced before the thorough test system is established to reduce the error.

**Table 4** Corrosion rates comparison between electrochemical test and mass loss method in 0.1 mol/L NaCl [70]

	Corrosion rate	Corrosion rate
Material	by electrochemical test/	by mass loss test/
	$(\text{mg}\cdot\text{d}^{-1}\cdot\text{cm}^{-2})$	$(\text{mg}\cdot\text{d}^{-1}\cdot\text{cm}^{-2})$
Mg	1214.5	142.8
Mg12Li	2	0.4
Mg1Ca	2.7	0.8
AZ31	102.8	12.5

#### 4 Conclusions

- 1) A more suitable in vitro corrosion system could be chosen to mimic the in vivo environment. Simulated body fluid containing the similar components to human blood plasma should be applied as electrolyte solution, such as SBF and culture medium with serum. Buffer system is preferred.
- 2) Surface roughness of metallic samples should be the same as implants to avoid man-made error.
- 3) Range of electrochemical parameters should be considered to reduce the shift of measured curves.
- 4) Ratio of solution volume to sample surface area should be adopted based on the real implant situation, lower ratio in vascular intervention material while higher ratio in orthopaedic implants.
- 5) Too long immersion time should be abandoned, because it is far away from the true situation after the cell adhesion.
  - 6) Dynamic corrosion is preferred and the shear

force or flow rate of the solution should also be chosen close to the in vivo condition.

7) As to the evaluation methodology of corrosion rate, the different methods may complement one another.

#### References

- [1] WITTE F, KAESE V, HAFERKAMP H, SWITZER E, MEYER-LINDENBERG A, WIRTH C J, WINDHAGEN H. In vivo corrosion of four magnesium alloys and the associated bone response [J]. Biomaterials, 2005, 26(17): 3557–3563.
- [2] XU L, YU G, ZHANG E, PAN F, YANG K. In vivo corrosion behavior of Mg-Mn-Zn alloy for bone implant application [J]. Journal of Biomedical Materials Research: Part A, 2007, 83(3): 703-711.
- [3] WAKSMAN R, PAKALA R, KUCHULAKANTI P K, BAFFOUR R, HELLINGA D, SEABRON R, TIO F O, WITTCHOW E, HARTWIG S, HARDER C. Safety and efficacy of bioabsorbable magnesium alloy stents in porcine coronary arteries [J]. Catheterization and Cardiovascular Interventions, 2006, 68(4): 607–617.
- [4] HE Y, TAO H R, ZHANG Y, JIANG Y, ZHANG S, ZHAO C, LI J, ZHANG B, SONG Y, ZHANG X N. Biocompatibility of bio-Mg-Zn alloy within bone with heart, liver, kidney and spleen [J]. Chinese Science Bulletin, 2009, 54(3): 484-491.
- [5] PEUSTER M, HESSE C, SCHLOO T, FINK C, BEERBAUM P, von SCHNAKENBURG C. Long-term biocompatibility of a corrodible peripheral iron stent in the porcine descending aorta [J]. Biomaterials, 2006, 27(28): 4955–4962.
- [6] PEUSTER M, WOHLSEIN P, BRÜGMANN M, EHLERDING M, SEIDLER K, FINK C, BRAUER H, FISCHER A, HAUSDORF G. A novel approach to temporary stenting: Degradable cardiovascular stents produced from corrodible metal-results 6–18 months after implantation into new zealand white rabbits [J]. Heart, 2001, 86(5): 563.
- [7] WAKSMAN R O N, PAKALA R, BAFFOUR R, SEABRON R, HELLINGA D, TIO F O. Short-term effects of biocorrodible iron stents in porcine coronary arteries [J]. Journal of Interventional Cardiology, 2008, 21(1): 15–20.
- [8] ZARTNER P, CESNJEVAR R, SINGER H, WEYAND M. First successful implantation of a biodegradable metal stent into the left pulmonary artery of a preterm baby [J]. Catheterization and Cardiovascular Interventions, 2005, 66(4): 590–594.
- [9] ERBEL R, DI MARIO C, BARTUNEK J, BONNIER J, de BRUYNE B, EBERLI F R, ERNE P, HAUDE M, HEUBLEIN B, HORRIGAN M. Temporary scaffolding of coronary arteries with bioabsorbable magnesium stents: A prospective, non-randomised multicentre trial [J]. The Lancet, 2007, 369(9576): 1869–1875.
- [10] DI MARIO C, GRIFFITHS H U W, GOKTEKIN O, PEETERS N, VERBIST J A N, BOSIERS M, DELOOSE K, HEUBLEIN B, ROHDE R, KASESE V. Drug-eluting bioabsorbable magnesium stent [J]. Journal of interventional cardiology, 2004, 17(6): 391–395.
- [11] SCHRANZ D, ZARTNER P, MICHEL-BEHNKE I, AKINTÜRK H. Bioabsorbable metal stents for percutaneous treatment of critical recoarctation of the aorta in a newborn [J]. Catheterization and Cardiovascular Interventions, 2006, 67(5): 671–673.
- [12] YANG L, ZHANG E. Biocorrosion behavior of magnesium alloy in different simulated fluids for biomedical application [J]. Materials Science and Engineering C, 2009, 29(5): 1691–1696.
- [13] SONG G L, ATRENS A. Corrosion mechanisms of magnesium alloys [J]. Advanced Engineering Materials, 2000, 1(1): 11–33.
- [14] LI Z, GU X, LOU S, ZHENG Y. The development of binary Mg-Ca alloys for use as biodegradable materials within bone [J].

- Biomaterials, 2008, 29(10): 1329-1344.
- [15] MORAVEJ M, PURNAMA A, FISET M, COUET J, MANTOVANI D. Electroformed pure iron as a new biomaterial for degradable stents: In vitro degradation and preliminary cell viability studies [J]. Acta Biomaterialia, 2010, 6(5): 1843-1851.
- [16] WITTE F, FEYERABEND F, MAIER P, FISCHER J, STÖRMER M, BLAWERT C, DIETZEL W, HORT N. Biodegradable magnesiumhydroxyapatite metal matrix composites [J]. Biomaterials, 2007, 28(13): 2163–2174.
- [17] KANNAN M B, RAMAN R K. In vitro degradation and mechanical integrity of calcium-containing magnesium alloys in modifiedsimulated body fluid [J]. Biomaterials, 2008, 29(15): 2306–2314.
- [18] KOKUBO T, TAKADAMA H. How useful is SBF in predicting in vivo bone bioactivity [J]. Biomaterials, 2006, 27(15): 2907–2915.
- [19] ALVAREZ-LOPEZ M, PEREDA M D, DEL VALLE J A, FERNANDEZ-LORENZO M, GARCIA-ALONSO M C, RUANO O A, ESCUDERO M L. Corrosion behaviour of AZ31 magnesium alloy with different grain sizes in simulated biological fluids [J]. Acta Biomaterialia, 2010, 6(5): 1763–1771.
- [20] YAO Z, LI L, JIANG Z. Adjustment of the ratio of Ca/P in the ceramic coating on Mg alloy by plasma electrolytic oxidation [J]. Applied Surface Science, 2009, 255(13-14): 6724-6728.
- [21] SONG Y W, SHAN D Y, HAN E H. Electrodeposition of hydroxyapatite coating on AZ91D magnesium alloy for biomaterial application [J]. Materials Letters, 2008, 62(17): 3276–3279.
- [22] XIN Y, JIANG J, HUO K, TANG G, TIAN X, CHU P K. Corrosion resistance and cytocompatibility of biodegradable surgical magnesium alloy coated with hydrogenated amorphous silicon [J]. Journal of Biomedical Materials Research: Part A, 2009, 89(3): 717–726
- [23] XIN Y, HUO K, TAO H, TANG G, CHU P K. Influence of aggressive ions on the degradation behavior of biomedical magnesium alloy in physiological environment [J]. Acta Biomaterialia, 2008, 4(6): 2008–2015.
- [24] ZHANG E, YIN D, XU L, YANG L, YANG K. Microstructure, mechanical and corrosion properties and biocompatibility of Mg-Zn-Mn alloys for biomedical application [J]. Materials Science and Engineering C, 2009, 29(3): 987–993.
- [25] YAMAMOTO A, HIROMOTO S. Effect of inorganic salts, amino acids and proteins on the degradation of pure magnesium in vitro [J]. Materials Science and Engineering C, 2009, 29(5): 1559–1568.
- [26] ZENG R, DIETZEL W, WITTE F, HORT N, BLAWERT C. Progress and challenge for magnesium alloys as biomaterials [J]. Advanced Engineering Materials, 2008, 10(8): B3–B14.
- [27] SONG G, SONG S. Corrosiion behavior of magnesium in simulated human body fluid [J]. Chinese Journal of Physical Chemistry, 2006, 22(10): 1222–1226.
- [28] HIROMOTO S, YAMAMOTO A, MARUYAMA N, SOMEKAWA H, MUKAI T. Influence of pH and flow on the polarisation behaviour of pure magnesium in borate buffer solutions [J]. Corrosion Science, 2008, 50(12): 3561–3568.
- [29] SONG G, SONG S. A possible biodegradable magnesium implant material [J]. Advanced Engineering Materials, 2007, 9(4): 298–302.
- [30] SHI P, NG W F, WONG M H, CHENG F T. Improvement of corrosion resistance of pure magnesium in Hanks' solution by microarc oxidation with sol–gel TiO<sub>2</sub> sealing [J]. Journal of Alloys and Compounds, 2009, 469(1): 286–292.
- [31] XU L, ZHANG E, YANG K. Phosphating treatment and corrosion properties of Mg-Mn-Zn alloy for biomedical application [J]. Journal of Materials Science: Materials in Medicine, 2009, 20(4): 859-867
- [32] XIN Y, LIU C, HUO K, TANG G, TIAN X, CHU P K. Corrosion behavior of ZrN/Zr coated biomedical AZ91 magnesium alloy [J]. Surface and Coatings Technology, 2009, 203(17–18): 2554–2557.

- [33] HÄNZI A C, GUNDE P, SCHINHAMMER M, UGGOWITZER P J. On the biodegradation performance of an Mg-Y-RE alloy with various surface conditions in simulated body fluid [J]. Acta Biomaterialia, 2009, 5(1): 162–171.
- [34] HILBERT L R, BAGGE-RAVN D, KOLD J, GRAM L. Influence of surface roughness of stainless steel on microbial adhesion and corrosion resistance [J]. International biodeterioration & biodegradation, 2003, 52(3): 175–185.
- [35] MARTIN J Y, SCHWARTZ Z, HUMMERT T W, SCHRAUB D M, SIMPSON J, Lankford Jr J, DEAN D D, COCHRAN D L, BOYAN B D. Effect of titanium surface roughness on proliferation, differentiation, and protein synthesis of human osteoblast-like cells (MG63) [J]. Journal of Biomedical Materials Research, 1995, 29(3): 389–401.
- [36] WITTE F, FISCHER J, NELLESEN J, CROSTACK H A, KAESE V, PISCH A, BECKMANN F, WINDHAGEN H. In vitro and in vivo corrosion measurements of magnesium alloys [J]. Biomaterials, 2006, 27(7): 1013–1018.
- [37] SONG Y, SHAN D, CHEN R, ZHANG F, HAN E H. Biodegradable behaviors of AZ31 magnesium alloy in simulated body fluid [J]. Materials Science and Engineering C, 2009, 29(3): 1039–1045.
- [38] GUAN Y C, ZHOU W, ZHENG H Y. Effect of laser surface melting on corrosion behaviour of AZ91D Mg alloy in simulated-modified body fluid [J]. Journal of Applied Electrochemistry, 2009, 39(9): 1457–1464
- [39] GU X, ZHENG Y, CHENG Y, ZHONG S, XI T. In vitro corrosion and biocompatibility of binary magnesium alloys [J]. Biomaterials, 2009, 30(4): 484–498.
- [40] ZHANG S, LI J, SONG Y, ZHAO C, ZHANG X, XIE C, ZHANG Y, TAO H, HE Y, JIANG Y. In vitro degradation, hemolysis and MC3T3-E1 cell adhesion of biodegradable Mg-Zn alloy [J]. Materials Science and Engineering C, 2009, 29(6): 1907-1912.
- [41] WANG Y M, WANG F H, XU M J, ZHAO B, GUO L X, OUYANG J H. Microstructure and corrosion behavior of coated AZ91 alloy by microarc oxidation for biomedical application [J]. Applied Surface Science, 2009, 255(22): 9124–9131.
- [42] PEREDA M D, ALONSO C, BURGOS-ASPERILLA L, DEL VALLE J A, RUANO O A, PEREZ P, FERNÁNDEZ LORENZO de MELE M A. Corrosion inhibition of powder metallurgy Mg by fluoride treatments [J]. Acta Biomaterialia, 2010, 6(5): 1772–1782.
- [43] YIN D S, ZHANG E L, ZENG S Y. Effect of Zn on mechanical property and corrosion property of extruded Mg–Zn–Mn alloy [J]. Transactions of Nonferrous Metals Society of China, 2008, 18(4): 763–768
- [44] XU L, ZHANG E, YIN D, ZENG S, YANG K. In vitro corrosion behaviour of Mg alloys in a phosphate buffered solution for bone implant application [J]. Journal of Materials Science: Materials in Medicine, 2008, 19(3): 1017–1025.
- [45] KIM W C, KIM J G, LEE J Y, SEOK H K. Influence of Ca on the corrosion properties of magnesium for biomaterials [J]. Materials Letters, 2008, 62(25): 4146–4148.
- [46] ZHANG E, HE W, DU H, YANG K. Microstructure, mechanical properties and corrosion properties of Mg–Zn–Y alloys with low Zn content [J]. Materials Science and Engineering A, 2008, 488(1): 102–111
- [47] HERMAWAN H, DUBÉ D, MANTOVANI D. Degradable metallic biomaterials: Design and development of Fe–Mn alloys for stents [J]. Journal of Biomedical Materials Research: Part A, 2010, 93(1): 1–11.
- [48] ZHU S, HUANG N, SHU H, WU Y, XU L. Corrosion resistance and blood compatibility of lanthanum ion implanted pure iron by MEVVA [J]. Applied Surface Science, 2009, 256(1): 99–104.
- [49] SCHINHAMMER M, HÄNZI A C, LÖFFLER J F, UGGOWITZER P J. Design strategy for biodegradable Fe-based alloys for medical applications [J]. Acta Biomaterialia, 2010, 6(5): 1705–1713.

- [50] LIU B, ZHENG Y F. Effects of alloying elements (Mn, Co, Al, W, Sn, B, C and S) on biodegradability and in vitro biocompatibility of pure iron [J]. Acta Biomaterialia, 2011, 7(3): 1407–1420.
- [51] HERMAWAN H, ALAMDARI H, MANTOVANI D, DUBÉ D. Iron-manganese: New class of metallic degradable biomaterials prepared by powder metallurgy [J]. Powder Metallurgy, 2008, 51(1): 38–45
- [52] JIA Z, LI X, DU C. The influence of potential sweep rate on the results of the electrode process kinetic parameters test [J]. Chinese Journal of Corrosion and Protection, 2010, 31(11): 830–832. (in Chinese)
- [53] CUI X. The influence of equivalent circuit element parameter value on ac impedance spectrum [J]. Chinese Journal of Hebei Normal University, 2002, 26(4): 376–380. (in Chinese)
- [54] ISO E N. 10993—15. Biological evaluation of medical devices-Part15: Identification and quantification of degradation products from metals and alloys [S]. 2000.
- [55] ASTM G31—72: Standard practice for laboratory immersion corrosion testing of metals [S]. West Conshohocken, PA: American Society of Testing and Materials, 2004, 3.
- [56] HORT N, HUANG Y, FECHNER D, STÖRMER M, BLAWERT C, WITTE F, VOGT C, DRÜCKER H, WILLUMEIT R, KAINER K U. Magnesium alloys as implant materials–Principles of property design for Mg–RE alloys [J]. Acta Biomaterialia, 2010, 6(5): 1714–1725.
- [57] WANG Q, TAN L, XU W, ZHANG B, YANG K. Dynamic behaviors of a Ca-P coated AZ31B magnesium alloy during in vitro and in vivo degradations [J]. Materials Science and Engineering B, 2011, 176(20): 1718-1726.
- [58] GEIS-GERSTORFER J, SCHILLE C, SCHWEIZER E, RUPP F, SCHEIDELER L, REICHEL H P, HORT N, NOLTE A, WENDEL H P. Blood triggered corrosion of magnesium alloys [J]. Materials Science and Engineering B, 2011, 176(20): 1761–1766.
- [59] SCHILLE C, BRAUN M, WENDEL H P, SCHEIDELER L, HORT N, REICHEL H P, SCHWEIZER E, GEIS-GERSTORFER J. Corrosion of experimental magnesium alloys in blood and PBS: A gravimetric and microscopic evaluation [J]. Materials Science and Engineering B, 2011, 176(20): 1797–1801.
- [60] YANG J X, JIAO Y P, CUI F Z, LEE I S, YIN Q S, ZHANG Y. Modification of degradation behavior of magnesium alloy by IBAD coating of calcium phosphate [J]. Surface and Coatings Technology, 2008, 202(22): 5733–5736.
- [61] CHEN Y, ZHANG S, LI J, SONG Y, ZHAO C, ZHANG X. Dynamic degradation behavior of MgZn alloy in circulating m-SBF [J]. Materials Letters, 2010, 64(18): 1996–1999.
- [62] LÉVESQUE J, HERMAWAN H, DUBÉ D, MANTOVANI D. Design of a pseudo-physiological test bench specific to the development of biodegradable metallic biomaterials [J]. Acta Biomaterialia, 2008, 4(2): 284–295.
- [63] ZHU S, HUANG N, XU L, ZHANG Y, LIU H, SUN H, LENG Y. Biocompatibility of pure iron: In vitro assessment of degradation kinetics and cytotoxicity on endothelial cells [J]. Materials Science and Engineering C, 2009, 29(5): 1589–1592.
- [64] WANG Y, WEI M, GAO J. Improve corrosion resistance of magnesium in simulated body fluid by dicalcium phosphate dihydrate coating [J]. Materials Science and Engineering C, 2009, 29(4): 1311–1316.
- [65] XIN Y, HU T, CHU P K. In vitro studies of biomedical magnesium alloys in a simulated physiological environment: A review [J]. Acta Biomaterialia, 2011, 7(4): 1452–1459.
- [66] GU X N, LI N, ZHENG Y F, RUAN L. In vitro degradation performance and biological response of a Mg–Zn–Zr alloy [J]. Materials Science and Engineering B, 2011, 176(20): 1778–1784.

- [67] SONG G, ATRENS A. Understanding magnesium corrosion—A framework for improved alloy performance [J]. Advanced Engineering Materials, 2004, 5(12): 837–858.
- [68] WITTE F, HORT N, VOGT C, COHEN S, KAINER K U, WILLUMEIT R, FEYERABEND F. Degradable biomaterials based on magnesium corrosion [J]. Current Opinion in Solid State and Materials Science, 2008, 12(5-6): 63-72.
- [69] ASTM G102-89: Standard practice for calculation of corrosion rates
- and related information from electrochemical measurements [S]. West Conshohocken, PA: American Society of Testing and Materials, 2004
- [70] YFANTIS D C, YFANTIS D K, ANASTASSOPOULOU J. In vitro corrosion behavior of new magneisum alloys for bone regeneration [C]//Proceedings of the 5th WSEAS International Conference on Environment, Ecosystems and Development. Venice, Italy, 2006: 20–22.

### 生物可降解金属材料体外腐蚀测试体系综述

甄 珍1,奚廷斐1,2,郑玉峰1,3

- 1. 北京大学 前沿交叉学科研究院,生物材料与组织工程中心,北京 100871;
  - 2. 温州医学院 信息工程学院, 温州 325035;
  - 3. 北京大学 工学院,材料科学与工程系,北京 100871

摘 要:随着生物可降解金属材料日益受到关注,大量的体外腐蚀测试体系被用来模拟其体内腐蚀行为。不同的测试体系具有其独特的优点和缺点。为建立一个合理的并且更接近体内真实情况的测试体系,对可降解金属材料的腐蚀机理和体外腐蚀测试体系进行总结。从电解质溶液的选择、样品表面粗糙度的影响、测试方法以及腐蚀速度的评价方法等几个方面进行阐述,得到以下初步结论:电解质溶液应该选择与体液成分接近的含有蛋白的缓冲模拟体液,样品表面粗糙度和溶液体积与样品表面积之比应该接近植入部位的实际要求,并且采用动态腐蚀测试方法,同时多种腐蚀速度评价方法应当相互参照。

关键词:生物可降解;金属材料;体外测试;镁;铁

(Edited by Chao WANG)